Available online at www.sciencedirect.com
SCIENCE DIRECT®
Catalysis Today 99 (2005) 179–186
CATALYSIS TODAY
www.elsevier.com/locate/cattod

Oxidation of *o*-xylene on mesoporous Ti-phosphate-supported VO_x catalysts and promoter effect of K^+ on selectivity

J. Jiménez-Jiménez[a], J. Mérida-Robles[a], E. Rodríguez-Castellón[a], A. Jiménez-López[a], M. López Granados[b], S. del Val[b], I. Melián Cabrera[b,1], J.L.G. Fierro[b,*]

[a]*Departamento de Química Inorgánica, Cristalografía y Mineralogía, Facultad de Ciencias, Universidad de Málaga, Campus de Teatinos, 29071 Málaga, Spain*
[b]*Instituto de Catálisis y Petroleoquímica, CSIC, Marie Curie, 2 Campus de Cantoblanco, 28049 Madrid, Spain*

Available online 15 December 2004

Abstract

The selective oxidation of *o*-xylene on catalysts based on mesoporous titanium phosphate-supported vanadium oxide has been studied. The catalysts were characterized by different physico-chemical techniques (XRD, XPS, N_2 isotherms, TPD of chemisorbed NH_3 and Raman spectroscopy). The conversion and yield to phthalic anhydride increased with vanadium oxide loading up to one theoretical monolayer. Beyond this point, no substantial improvement was achieved. Moreover, a significant improvement in the yield of phthalic anhydride, coinciding with a decrease in the formation of carbon oxides, was observed when potassium was incorporated to the vanadium catalysts. The enhancement of the phthalic anhydride yield was correlated with the neutralization of the stronger surface acid centers by the K^+ ions, providing evidence for the hypothesis that stronger acid sites are involved in the formation of total oxidation products (carbon oxides).

Keywords: Vanadia catalysts; Ti-phosphates; *o*-Xylene oxidation; Phthalic anhydride

1. Introduction

In 1992, Mobil Oil scientists obtained new mesoporous materials named M41S [1]. The synthesis of such materials was carried out using surfactant molecules as template agents, giving rise to organic–inorganic mesostructures. Three geometries can be obtained with this synthetic methodology: lamellar, cubic and hexagonal. In the case of the latter two arrays, when organic molecules are removed the inorganic frameworks are preserved and porous materials are obtained. In the case of the lamellar structure, however, when surfactant molecules are removed the structure collapses, and a non-porous material is obtained. For this reason, most work has been developed with the cubic and hexagonal phases and research into synthesis has focused mainly on the collection of mesoporous silica doped with different elements with a view to improving the acidity of these solids, which have found applications as catalysts, catalyst supports, and adsorbent materials [2,3].

Other inorganic solids, such as metal oxides and metal(IV) phosphates, can also be obtained with this mesostructure type. In fact, the preparation of mesoporous zirconium phosphates by condensation of phosphoric acid and zirconium species with surfactant molecules has been reported [4]. In this case, when surfactant molecules are removed, mesoporous materials are also obtained. In a similar way, more recently mesoporous titanium(IV) phosphate materials have been obtained [4]; their textural and acid properties were also studied, revealing their potential application as acid solid catalysts. Finally, owing to their textural and acid properties these materials can also be used as supports of others catalytically active inorganic species.

Vanadium(V) oxide supported on titanium(IV) oxide (anatase) is one of the best catalytic systems for the selective

* Corresponding author. Tel.: +34 91 585 4769; fax: +34 91 585 4760.
E-mail address: jlgfierro@icp.csic.es (J.L.G. Fierro).
[1] Present address: Delft University of Technology, R&CE, DelftChemTech, Julianalaan 136, 2628 BL Delft, The Netherlands.

0920-5861/$ – see front matter © 2004 Elsevier B.V. All rights reserved.
doi:10.1016/j.cattod.2004.09.038

oxidation of *o*-xylene and toluene to phthalic anhydride [5,6]. This substance has an important added value, and its industrial synthesis is of current economical importance because phthalic anhydride (PA) is widely employed as a raw material in industrial processes [7–9].

This V_2O_5 supported on the anatase system has been largely characterized [10–12], and it has also been reported that the industrial catalyst contains phosphorous [7,13]. There is some controversy in the literature as to whether P should be considered an impurity, a promoter, or a poison. Actually, industrial catalysts present better yields when phosphate species are present, and several patents claim that the incorporation of phosphorous on the surface is beneficial for the catalytic properties [14]. Recently, layered α-titanium(IV) phosphate has been used as a support of vanadium(V) oxide as a catalyst for the oxidation of toluene and *o*-xylene [15], showing reasonable partial oxidation properties. Taking these aspects into consideration, the use of vanadium(V) oxide supported on mesoporous titanium(IV) phosphate as a catalyst for the selective oxidation reaction of *o*-xylene to phthalic anhydride seems worthy of exploration. It is expected that the higher specific surface area of this new support should improve activity.

By contrast, when alkaline elements are loaded into the V_2O_5/TiO_2 catalyst the catalytic properties of the systems are substantially modified [16,17]. The incorporation of alkaline ions such as K^+ may result in a decrease in surface acidity, since acid sites are neutralized [18,19]. The PA yield is improved because acid sites promote deep oxidation [15]. However, when a high amount of potassium is added, potassium vanadate can be also obtained on the catalyst surface [19–21].

Here, we report the characterization of mesoporous titanium phosphate-supported VO_x catalysts, their catalytic activity for the selective oxidation of *o*-xylene, and the effect of the incorporation of K^+ on the yield of PA.

2. Experimental

2.1. Catalyst preparation

The synthesis of vanadium(V) oxide supported on mesoporous titanium phosphate can be summarized in three steps: (i) synthesis of mesoporous titanium(IV) phosphate, (ii) wet-impregnation of the mesoporous phosphate with different amounts of vanadium(V), and (iii) calcination of catalysts. Mesoporous titanium(IV) phosphate was prepared by a sol–gel methodology as described elsewhere [4]. Surfactant molecules used as template were removed by heating in air at 823 K. The specific surface area of the support was 100 m^2/g.

Catalysts containing a theoretical loading of 2, 5, 10 and 20 wt.% of V_2O_5 were prepared by wet-impregnation of the mesoporous titanium(IV) phosphate, using an ethanolic solution prepared by adding V_2O_5 to an aqueous solution of oxalic acid at 323 K (2.3 g oxalic acid dihydrate/g V_2O_5). The impregnation solution was added to the mesoporous titanium phosphate and the excess of ethanol was removed by evaporation at 333 K in air. The precursors are referred to as *x*V–TiP, where *x* indicates the expected wt.% of V_2O_5 added during the preparation procedure. The precursors were then calcined at 823 K in air for 5 h and the catalysts obtained were designated *x*V–TiPc. It should be noted that for the catalyst containing 10% V_2O_5 a theoretical monolayer of V_2O_5 is formed, as calculated by geometric considerations [5] and assuming that the whole of the support area is available to disperse vanadium(V) oxide.

Potassium-containing catalysts were prepared by the addition of a KNO_3/water solution to the 5V–TiPc and 10V–TiPc materials. The amount of potassium added by wet-impregnation was equal to the value of the surface acidity of the catalysts (mol NH_3/g of catalyst) as determined by NH_3-TPD. After calcination in air at 723 K, potassium-containing solids were designated K*x*V–TiPc.

2.2. Catalyst characterization

The analysis of Ti and V was carried out by atomic absorption spectroscopy and P was determined colorimetrically [22]. XRD patterns were recorded on a Siemens D501 diffractometer (Cu Kα radiation) provided with a graphite monochromator. X-ray photoelectron spectroscopy (XPS) analyses were carried out using a Physical Electronics PHI 5700 spectrometer with non-monochromatic Mg Kα radiation (300 W, 15 kV, 1253.6 eV) as the excitation source. High-resolution spectra were recorded in the constant pass energy mode at 29.35 eV, using a 720 μm diameter analysis area. Under these conditions, the Au $4f_{7/2}$ line was recorded with 1.16 eV FWHM at a binding energy of 84.0 eV. The spectrometer energy scale was calibrated using Cu $2p_{3/2}$, Ag $3d_{5/2}$ and Au $4f_{7/2}$ photoelectron lines at 932.7, 368.3 and 84.0 eV, respectively. Charge referencing was carried out against adventitious carbon (C 1s 284.8 eV). C 1s and V 2p regions were first irradiated for 10 min to avoid the photoreduction of V(V) to V(IV). The pressure in the analysis chamber was maintained at less than 5×10^{-6} Pa. The PHI ACCESS ESCA-V6.0 F software package was used for data acquisition and analysis. A Shirley-type background was subtracted from the signals.

Thermogravimetric analyses were carried out on a Setaram Instrumentation apparatus. Samples (ca. 30 mg) were loaded and heated under a flow of synthetic air at a heating rate of 10 K/min at 1273 K. N_2 adsorption–desorption isotherms at 77 K were obtained using a Micromeritics ASAP 2000 apparatus. Samples were previously outgassed at 413 K for 24 h. Ammonia thermal programmed desorption (NH_3-TPD) was used to determine the total acidity of the samples. Before the adsorption of

ammonia at 373 K, the samples were heated at 773 K in a He flow. NH_3-TPD was performed between 373 and 773 K, at a heating rate of 10 K/min, and analyzed by a TC detector.

Raman spectra were recorded on a Renishaw 1000 spectrophotometer equipped with a cooled CCD detector (200 K) and a holographic Notch filter that removes elastic scattering. Samples were excited with the 514 nm Ar line. All samples were pretreated in situ in 100 mL/min (STP) of air at 673 K for 30 min in an in situ cell (Linkan, TS-1500) before recording the spectra (which were collected at 473 K under a flow of air).

2.3. Catalytic measurements

Catalytic activity measurements were carried out in a plug-flow glass fixed-bed reactor heated with a cylindrical oven. The catalyst mass used was 250 mg (W/F = 179 g s/L) diluted seven times in carborundum (particle size of both 0.42–0.50 mm). Gas flows were controlled by mass flow controllers. *o*-Xylene was fed as liquid with a perfusion pump. The O_2 and *o*-xylene molar concentrations in the feed were 0.8 and 20.8%, respectively (balance N_2). The inlet line was heated at 453 K to ensure the evaporation of alkylaromatics. A gas chromatograph (Varian Star 3400 CX) was connected on-line with the reactor outlet to analyze permanent gases and the volatile fraction of the reaction mixture. An ice bath was placed between the reactor outlet and the gas chromatograph to condense part of the reaction products and part of the unreacted *o*-xylene. The GC was equipped with TCD and FID detectors. Permanents gases (O_2, N_2, H_2O, CO and CO_2) and the gas fraction of organic compounds were analyzed by on-line injections. Additional information can be consulted elsewhere [15]. The carbon balance for most of the catalysts was 100% (within the experimental error) in all cases and at all temperatures. However, in the case of sample 20V–TiPc a deposit of heavy products was observed at the bottom of the reactor for high conversion values, slightly reducing the carbon balance for this sample.

3. Results

3.1. X-ray diffraction (XRD)

The support, mesoporous titanium(IV) phosphate, exhibited a diffraction line at 41 Å that can be assigned to d_{100} reflection. However, after wet-impregnation and subsequent calcination, this peak disappeared. In all cases, the XRD powder patterns for the *x*V–TiP samples, obtained after wet-impregnation of the support and calcination at 823 K do not show any diffraction peak, this process gives rise a lost of order due to the formation of smaller packets and the reflection line at low angle disappears. However, the textural properties of these materials are maintained. For calcined materials, only the XRD pattern of the sample with the highest vanadium content (20V–TiPc) showed reflection lines that corresponded to vanadium(V) oxide (see Fig. 1) indicating a good dispersion of vanadium species on the support surface for the low V loading catalysts. The corresponding K-promoted samples showed similar XRD patterns.

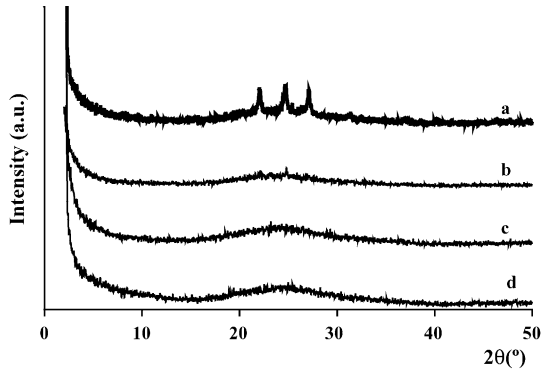

Fig. 1. XRD patterns of precursor: (a) 20V–TiP, (b) 10V–TiP, (c) 5V–TiP and (d) 2V–TiP; XRD patterns of catalysts: (a) 20V–TiPc, (b) 10V–TiPc, (c) 5V–TiPc and (d) 2V–TiPc.

3.2. Photoelectron spectroscopy (XPS)

Nogier and Delamar [23] detected large discrepancies when the V_2O_5/TiO_2 system was studied by XPS by different laboratories, and some of their recommendations to improve the reproducibility of the XPS measurements have been followed. The surface V/Ti atomic ratios of the samples studied was determined by XPS analysis and the ''bulk'' V/Ti atomic ratio was evaluated by elemental chemical analysis. Fig. 2 compares the bulk and the surface V/Ti atomic ratios as a function of the V_2O_5 loading. The surface and bulk V/Ti atomic ratios are only similar in the case of the 2V–TiPc sample. When the percentage of added vanadium increased, the surface V/Ti atomic ratio was always much higher than those of the bulk, above all for the 20V–TiPc catalyst. In this catalyst, vanadium(V) oxide was not very well dispersed because discrete crystallites of V_2O_5 were

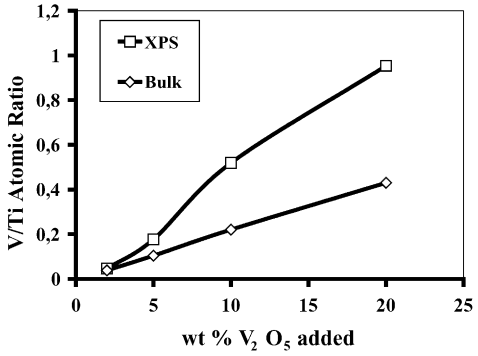

Fig. 2. XPS and V/Ti atomic ratio of different catalysts.

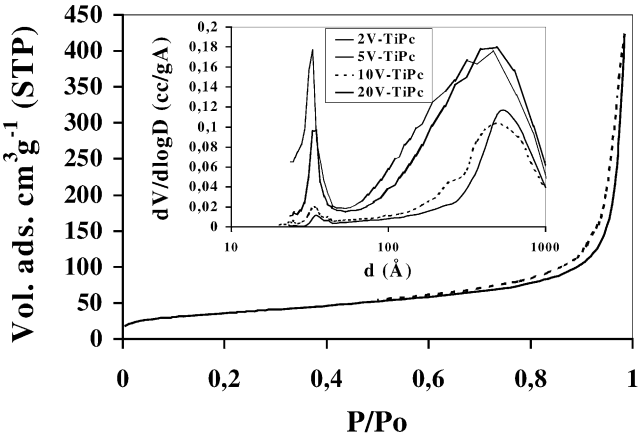

Fig. 3. Pore size distribution of different *x*V–TiPc materials. Onset: adsorption–desorption isotherm of N_2 at 77 K of 10V–TiPc catalyst.

detected by XRD, instead of the development of several monolayers of amorphous V_2O_5 spread over the surface of the support. The V 2p signals for the samples studied, after satellite subtraction, were very similar, a symmetric V $2p_{3/2}$ peak being observed at 517.3–517.0 eV; this was assigned to the exclusive presence of V(V), mainly as vanadium(V) oxide.

3.3. Specific BET area and porosity

The N_2 adsorption–desorption isotherms (77 K) of the catalysts studied were of type IV (IUPAC classification) typical of mesoporous solids. Fig. 3 shows the isotherm for 10V–TiPc as a representative example. (The peak at ca. 20 Å in the pore size distribution curves represented in the inset that appears in the low V loading samples arises from the tensile strength effect and are not an indication of microporosity.) The incorporation of vanadium(V) oxide gave rise to a dramatic reduction in the BET area from 100 (support) to 8.3 m^2/g in the case of the sample with the highest vanadium content (20V–TiPc). The rest of the catalysts had specific areas of 63, 33 and 13 m^2/g for 2V–TiPc, 5V–TiPc and 10V–TiPc, respectively. The incorporation of vanadium(V) oxide also modified the pore size distribution (Fig. 3), because the vanadium(V) oxide phase was filling the pores of the mesoporous titanium(IV) phosphate. The addition of K did not significantly modify the textural properties.

3.4. Raman spectra

Raman spectra were recorded for the TiP support and for the *x*V–TiPc series of catalysts and are shown in Fig. 4. The spectrum of the bare support (TiPc) shows Raman bands at 1080, 1020, 824, 626, 436 and 300 cm^{-1} (●), so these bands must arise form the support. The 2V–TiPc and 5V–TiPC materials show the same vibrations in the Raman spectra, i.e., the active phase was not detected. This does not mean that vanadium had migrated to the bulk and that vanadium oxide species were not present at the surface of the support: the XPS results indicated that their V/Ti surface ratios were higher than the bulk V/Ti values, indicating that V is concentrated at the surface of the solid. It is likely that the bands of the V species would not be detected by Raman because they are overshadowed by the most intense Raman bands of the support. The spectrum of 10V–TiPc showed new bands, which were assigned to vanadium(V) oxide species. However, the obtained spectra were different when diverse grains of sample were spotted, which means that a heterogeneous distribution of vanadium species on the support exists. Basically, three types of grains were observed. In one type of grains, Raman bands of support (●) are only present. For other grains, besides the support bands, other bands were observed at 993, 702, 525, 476, 404, 300, 283, 192 and 168 cm^{-1}(▲). These bands were assigned to vanadium(V) oxide [13]. A third type showed additional bands at 1028, 870, 800, 650, 600 and 350 cm^{-1}(×), which can be assigned to polymeric vanadium species (VO_x) [24–26]. The possibility that monomeric vanadium species is present on the support cannot be discarded since it presents a unique band at slightly higher frequencies than 1030 cm^{-1} and it can be overshadowed by the corresponding V=O vibration of the polymeric species. For the 20V–TiPc catalysts, two grain types were present: one whose Raman spectrum showed the same bands as the support (●) and the other in which the V_2O_5 bands (▲) were also present.

3.5. Surface acidity

NH_3-TPD was used to evaluate the number of surface acid sites. The Ti phosphate surface is expected to expose P–OH and Ti–OH groups with a Brønsted character and also Ti coordinatively unsaturated sites with a Lewis character. The histograms shown in Fig. 5 correspond to the total acidity and the number of acid sites desorbed at different temperature ranges for the catalysts studied. The total acidity significantly decreased due to increasing percentages of vanadium: from 851 to 379 μmol NH_3/g desorbed for 2V–TiPc and 20V–TiPc, respectively. This reduction was not uniform for the different temperature ranges. Thus, the decrease was more significant for the weaker acid sites, corresponding to ammonia desorbed between 473 and 673 K. However, for the strong acid sites, this reduction was less important, which means that vanadium incorporation leaves the stronger acid sites fairly intact; supposedly the P–OH groups. By contrast, when potassium was added, besides the milder acid centers the stronger acid sites were also neutralized. Moreover, the total acidity decreased dramatically: six times for 5V–TiPc (from 609 to 111 μmol/g) and close to ten times for the 10V–TiPc material (from 379 to 40 μmol/g). It is clear that the incorporation of K remarkably suppresses the acidity of the surface by neutralizing the whole strength range of the acid sites.

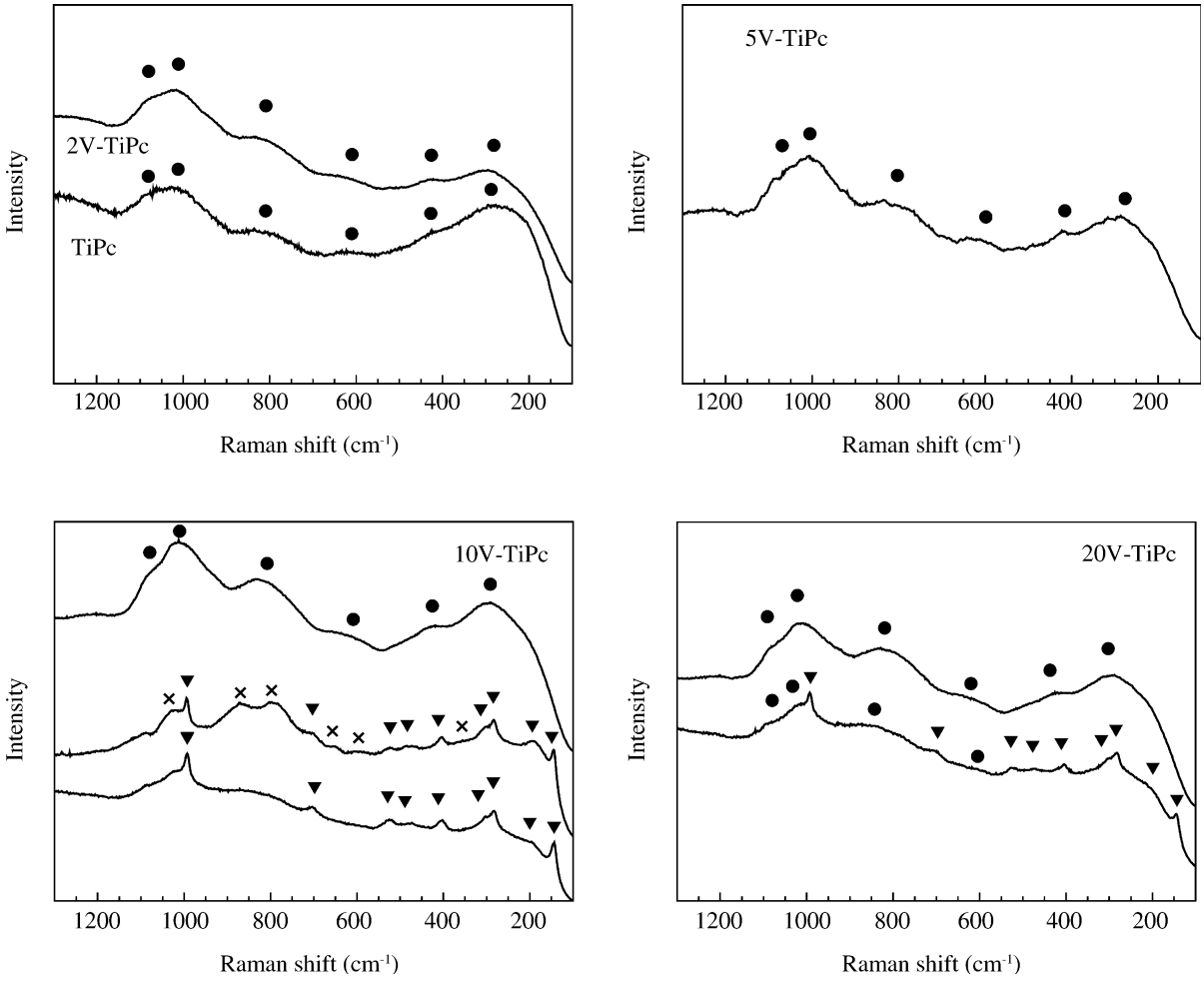

Fig. 4. Raman spectra of the catalysts (see text for the assignation of the bands).

3.6. Catalytic activity

Figs. 6 and 7 show the catalytic results for the oxidation of *o*-xylene on the set of the catalysts studied at different temperatures. *o*-Xylene was converted to partially oxidized products such as *o*-tolualdehyde (*o*-TAL), phthalic anhydride (PA), phthalide (PL) as major products. The product of greatest interest is PA, for this reason a good catalyst must exhibit high selectivity to this product in the oxidation of *o*-xylene. Catalytic performance was improved with the incorporation of vanadium with respect to the bare support. Thus, the presence of vanadium in the catalysts elicited an important increase in *o*-xylene conversion. This was most evident in the cases of samples 2V–TiPc and 5V–TiPc, where the increase in the vanadium percentage in the catalyst markedly enhanced the conversion of *o*-xylene (Fig. 6a). However, for the samples with a vanadium loading higher than 5 wt.%—samples 10V–TiPc and 20V–TiPc—the observed conversion values were not substantially higher than those of the 5V–TiPc. The non-homogeneous distribution of vanadium species and the appearance of V_2O_5 microcrystals on the catalysts with the higher loadings did not contribute to an improvement in catalytic conversion. The selectivity to PA for the different catalysts studied is shown in Fig. 6b. The bare mesoporous titanium(IV) phosphate (support) showed the lowest

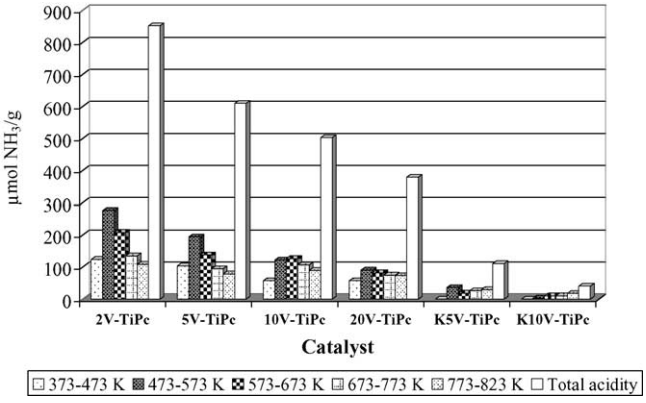

Fig. 5. Total acidity of *x*V–TiPc catalyst from temperature programmed desorption of ammonia.

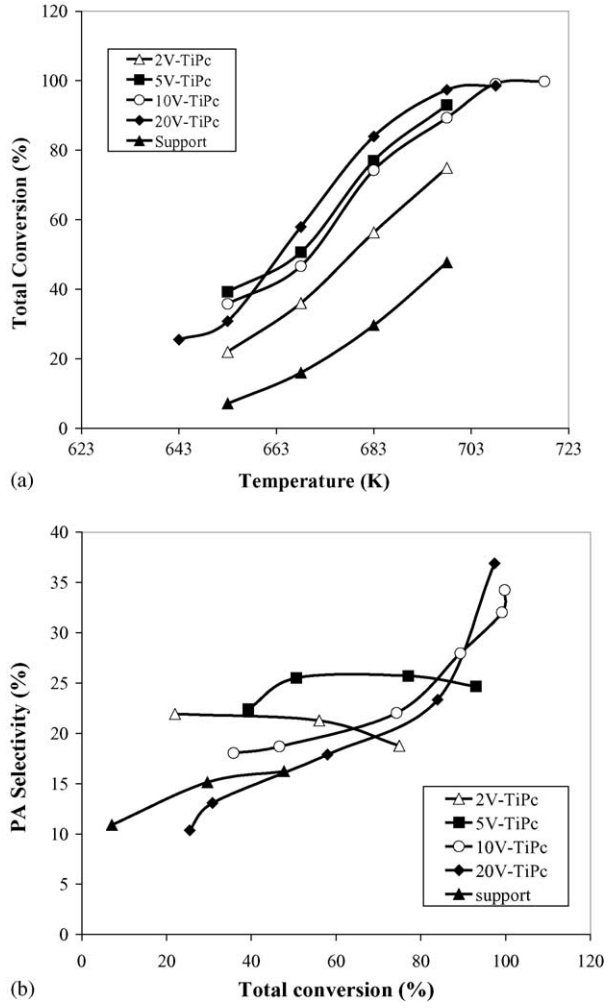

Fig. 6. (a) *o*-Xylene conversion for *x*V–TiPc catalysts and support; (b) selectivity to PA of different studied catalysts.

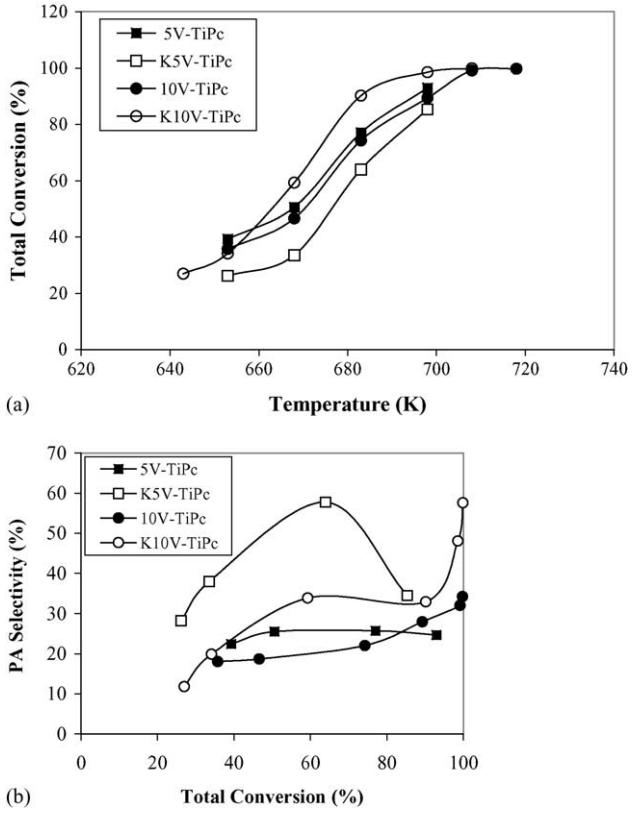

Fig. 7. (a) *o*-Xylene conversion and (b) selectivity to PA for 5V–TiPc and 10V–TiPc catalysts and respective K^+ exchanged materials.

selectivity to PA and the highest selectivity to CO and CO_2. Toluene and benzene (cracking products) were also obtained. For the vanadium-containing catalysts, two types of profiles were observed. For the 2V–TiPc and 5V–TiPc samples, selectivity to PA increased smoothly when conversion decreased whereas for samples 10V–TiPc and 20V–TiPc there was a remarkable increase in the yield to PA at higher conversion values.

The addition of potassium, which neutralizes acid sites, slightly modified the total conversion of *o*-xylene for the K5V–TiPc sample (see Fig. 7a). Actually, it had slightly lower conversion values than those of the potassium-free catalysts. In contrast, a clear enhancement was observed for the catalyst with 10 wt.% of V_2O_5 (K5V–TiPc). Nevertheless, the most remarkable result was that the addition of K^+ produced a higher PA yield in the two catalysts studied. In one case—K5V–TiPcc—the improvement was clear at medium conversion, whereas in the K10V–TiPc sample PA yield was especially high at larger conversion. The PA yield of K10V–TiPc was lower to that found in the V/TiO_2 systems (higher than 80%), the so far best reported catalyst [12].

4. Discussion

It is well known that in the case of VO_x–TiO_2 catalysts, for loadings less than the monolayer, the deposit consists of mono- and polyvanadates; beyond this limit V_2O_5 appears [27]. Wet-impregnation of mesoporous titanium(IV) phosphate with variable amounts of vanadium gives rise to catalysts with reasonably good properties for oxidation reactions. However, one observation that should be kept in mind is that use of the wet-impregnation method for vanadium incorporation gives rise to a non-homogeneous deposition of the vanadium species on the surface of support, especially for high vanadium loadings, as deduced from the XRD and Raman spectral data. Thus, the XRD powder patterns of sample 20V–TiPc (Fig. 1) show the diffraction peaks of vanadium(V) oxide, although this loading only represents twice the theoretical amount corresponding to a monolayer of V_2O_5. This means that part of the vanadium in the sample is aggregated, forming V_2O_5 crystals. The Raman results show that the situation is similar in the 10V–TiPc sample, although in this case part of the vanadium is also present as polymeric species. The V_2O_5 aggregates are larger in the 20V–TiPc sample and are visible by XRD, whereas their size in the 10V–TiPc sample is smaller and they are undetectable by XRD. A direct consequence of the formation of these aggregates is the occlusion of pores in the

support and, as a consequence, the BET areas decrease steadily with V_2O_5 loading. It is clear that improvements in the method used for incorporation is required to achieve better dispersion of the vanadium oxide phase and hence better catalytic properties; this should encourage the search for a better method of vanadium incorporation. In the case of VO_x–TiO_2 systems, the maximum dispersion is obtained by grafting in anhydrous media or by adsorption of $VO_2(OH)_2^-$ at pH 5.5 on anatase [28].

Regarding catalytic activity, the incorporation of low amounts of vanadium (2V–TiPc and 5V–TiPc) results in an increase in the conversion of *o*-xylene. For catalysts with V_2O_5 percentages higher than 5%, the conversion curves are similar and no improvements are achieved. This can be explained in terms of two opposite effects: the increase in V_2O_5 loading is balanced by the decreasing specific BET surface area. In addition, as the vanadium loading increases, vanadium sites exposed to the gas phase does not increase in a proportional manner, since larger crystallites of V_2O_5 are formed.

With respect to the selectivity to PA, two profiles were observed (Fig. 6b). In the case of the samples with lower V_2O_5 percentages (2V–TiPc and 5V–TiPc), the selectivity to PA decreases smoothly as conversion become higher. However, for samples with higher V_2O_5 percentages, the selectivity to PA increases remarkably at higher conversion. This may be due to the deep oxidation reaction of *o*-xylene and of the partial oxidation products to CO and CO_2. The presence of strong acid sites on the catalyst may contribute to the deep oxidation reaction, and catalysts with a significant number of acid sites (i.e., with low V_2O_5 percentages) show the higher selectivity to CO and CO_2, in detriment to lower PA yield. The catalysts with the highest loading (10 and 20 wt.% of V_2O_5), which exhibit the lowest acidity, favor the formation of partial oxidation products, and hence when conversion increases the selectivity to PA follows the same trend.

Moreover, only in the case of the 10V–TiPc catalyst are the bands characteristic of polymeric vanadium species detected. As indicated above, it is very likely that these species would also exist at the surface of the 2V–TiPc and 5V–TiPc samples, although but they would be hidden by the more intense support Raman bands. The presence of these species is important because some authors have suggested that they could be involved in the selective partial oxidation of *o*-xylene [13], explaining the relatively high yield values (34.2%) to PA obtained with these catalysts. For 20V–TiPc, although the amount of vanadium loaded was twice that for the 10V–TiPc sample, the PA yield is only slightly higher because the additional incorporation of V does not result in homogeneous spreading of the vanadium oxide but, instead, in the formation of large V_2O_5 crystals (with a relatively lower specific surface area), which contributes to selective oxidation improvement being almost negligible.

The involvement of acid sites in the selective oxidation of *o*-xylene is seen in the fact that the incorporation of K^+ gave rise to a remarkable improvement in the PA yield in the two catalysts studied. Although the PA yield-conversion patterns are different (which very probably reflects complex reactions between the vanadium oxide species, the potassium sites, and the partial oxidation pathways), it is clear that neutralization of the acid sites causes a depletion of the total oxidation of intermediates, thereby favoring the partial oxidation products.

5. Conclusions

Vanadium(V) oxide supported on mesoporous titanium phosphate can be used as a catalyst in the partial oxidation of *o*-xylene to phthalic anhydride. The results indicate that the incorporation of vanadium(V) oxide using a wet-impregnation method enhanced the catalytic properties of the bare support. However, improvements in the incorporation method of the vanadium must be achieved to upgrade vanadium oxide dispersion and the PA yield. Moreover, the addition of K^+ to neutralize the acid sites still exposed at the surface of the catalysts resulted in a remarkable increase in the selectivity and hence in the yield of phthalic anhydride. This improvement in the PA yield was more evident in the 20V–TiPc catalyst, whose PA yield was closer to the well-known better system for *o*-xylene oxidation: V/TiO_2. This latter result supports the hypothesis that strong acid sites are involved in the total oxidation of the products coming from the partial oxidation of *o*-xylene to carbon oxides.

References

[1] J.S. Beck, J.C. Vartuli, W.J. Roth, M.E. Leonowicz, C.T. Kresge, K.D. Schmitt, C.T.-W. Chu, D.H. Olson, E.W. Sheppard, S.B. McCullen, J.B. Higgins, J.C. Schlenker, J. Am. Chem. Soc. 114 (1992) 10834.
[2] A. Corma, Chem. Rev. 95 (1995) 559;
A. Sayari, Chem. Mater. 8 (1996) 1840.
[3] J. Jiménez Jiménez, P. Maireles Torres, P. Olivera Pastor, E. Rodríguez Castellón, A. Jiménez López, D.J. Jones, J. Rozière, Adv. Mater. 10 (1998) 812.
[4] D.J. Jones, G. Aptel, M. Brandhorst, M. Jacquin, J. Jiménez Jiménez, A. Jiménez López, P. Maireles Torres, I. Piwonski, E. Rodríguez Castellón, J. Zajac, J. Rozière, J. Mater. Chem. 10 (2000) 1957.
[5] G. Centi, Appl. Catal. 147 (1996) 267.
[6] C.R. Dias, M. Farinha Portela, Catal. Rev. Sci. Eng. 39 (1997) 169.
[7] V. Nikolov, D. Klisurski, A. Anastasov, Catal. Rev. Sci. Eng. 33 (1991) 319.
[8] E.K. Gamstedt, M. Skivfars, T.K. Jacobsen, R. Pyrz, Composites 33 (2002) 1239.
[9] W.F. Su, Y.C. Lee, W.P. Pan, Therm. Acta 395 (2003) 395.
[10] G. Centi, D. Pinelli, F. Trifirò, J. Mol. Catal. 59 (1990) 221.
[11] G. Golinelli, F. Trifirò, Catal. Today 20 (1994) 153.
[12] B. Grzybowska-Swierkosz, Appl. Catal. A: Gen. 157 (1997) 263.
[13] S.L.T. Andersson, J. Chem. Soc., Faraday Trans. I 1537 (1986).
[14] T. Sato, Y. Nakanishi, K. Maruyama, T. Suzuki, US Patent 4,481,304 (1984) to Nippon Shok. Kag. Kog. Co.
[15] S. del Val, M. López Granados, J.L.G. Fierro, J. Santamaría González, A. Jiménez López, J. Catal. 188 (1999) 203.
[16] M.G. Nobbenhuis, P. Hug, T. Mallat, A. Baiker, Appl. Catal. A 180 (1994) 241.

[17] J. Zhu, S.L.T. Andersson, J. Chem. Soc., Faraday Trans. 85 (1989) 3629.
[18] L. Lietti, P. Forzati, G. Ramis, G. Busca, F. Bregan, Appl. Catal. B: Environ. 3 (1993) 13.
[19] R. Grabowsski, B. Grzybowska, A. Kozlowska, A. Sloczynski, K. Wcislo, Y. Barbaux, Top. Catal. 3 (1996) 277.
[20] D. Courcot, B. Grzybowska, Y. Barbaux, M. Rigole, A. Ponchel, M. Guelton, J. Chem. Soc., Dalton Trans. 92 (1996) 1609.
[21] D. Bulushev, L. Kiwi-Minsker, V.I. Zaikovskii, O.B. Lapina, A.A. Ivanov, S.I. Reshetnikov, A. Renken, Appl. Catal. A: Gen. 202 (2000) 243.
[22] G. Alberti, P. Cardini Galli, U. Costantino, E. Torraca, J. Inorg. Nucl. Chem. 29 (1967) 571.
[23] J.Ph. Nogier, M. Delamar, Catal. Today 20 (1994) 109.
[24] J.M. Jehng, G. Deo, B.M. Weckhuysen, I.E. Wachs, J. Mol. Catal. A: Chem. 110 (1996) 41.
[25] M.A. Vuurman, I.E. Wachs, J. Phys. Chem. 96 (1992) 7008.
[26] G. Deo, I.E. Wachs, J. Catal. 146 (1994) 335.
[27] I.E. Wachs, L.E. Briand, J.M. Jehng, L. Burcham, X. Gao, Catal. Today 57 (2000) 323.
[28] F. Chilker, J.Ph. Nogier, J.L. Bonardet, Catal. Today 78 (2003) 139.